Inorganic Chemistry

Article

pubs.acs.org/IC

Galactodendritic Porphyrinic Conjugates as New Biomimetic Catalysts for Oxidation Reactions

Kelly A. D. F. Castro,[†] Sandrina Silva,[‡] Patrícia M. R. Pereira,[‡] Mário M. Q. Simões,[‡] Maria da Graça P. M. S. Neves,[‡] José A. S. Cavaleiro,[‡] Fernando Wypych,[†] João P. C. Tomé,[#,‡,§] and Shirley Nakagaki*[,†]

[†]Laboratório de Química Bioinorgânica e Catálise, Universidade Federal do Paraná (UFPR), CP 19081, CEP 81531-990, Curitiba, Paraná Brazil

[‡]Department of Chemistry and QOPNA, University of Aveiro, 3810-193 Aveiro, Portugal

[§]Department of Organic and Macromolecular Chemistry, Ghent University, B-9000 Gent, Belgium

S *Supporting Information*

ABSTRACT: This work employed [5,10,15,20-tetrakis-(pentafluorophenyl)porphyrin] ([H_2(TPPF$_{20}$)], **H_2P1**) as the platform to prepare a tetrasubstituted galactodendritic conjugate porphyrin (**H_2P3**). After metalation with excess copper(II) acetate, **H_2P3** afforded a new solid porphyrin material, **Cu_4CuP3S**. This work also assessed the ability of the copper(II) complex (**CuP3**) of **H_2P3** to coordinate with zinc(II) acetate, to yield the new material **Zn_4CuP3S**. UV−visible, Fourier transform infrared, and electron paramagnetic resonance spectroscopies aided full characterization of the synthesized solids. (*Z*)-Cyclooctene epoxidation under heterogeneous conditions helped to evaluate the catalytic activity of **Cu_4CuP3S** and **Zn_4CuP3S**. The efficiency of **Cu_4CuP3S** in the oxidation of another organic substrate, catechol, was also investigated. According to the results obtained in the heterogeneous process, **Cu_4CuP3S** mimicked the activity of cytochrome P-450 and catecholase. In addition, **Cu_4CuP3S** was reusable after recovery and reactivation. The data obtained herein were compared with the results achieved for the copper complex (**CuP1**) of [H_2(TPPF$_{20}$)] and for **CuP3** under homogeneous conditions.

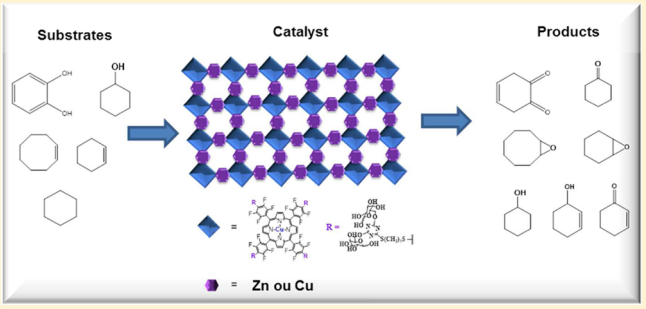

1. INTRODUCTION

The development of selective, highly efficient, and easily recoverable and reusable catalysts for oxidation reactions has become one of the main targets of modern chemistry. Porphyrins and other macrocyclic compounds have found frequent application in this field.

Porphyrins play an important role as functional molecules in a wide variety of biological systems. For this reason, they have attracted considerable interest from the scientific community. Among the extensive biological and chemical properties of porphyrins is their ability to act as versatile ligand for an array of transition metal ions. The resulting complexes generally present good catalytic activity.[1,2]

Inspired by biological systems, researchers have concentrated efforts on the design and development of new synthetic routes that can afford original porphyrins and metalloporphyrins[3] for a number of different purposes,[4−6] such as biological applications[7−10] and use in catalysis,[11−16] sensors,[17,18] and solar cells.[19,20]

Over the last 30 years, many literature papers have reported that synthetic porphyrins and their Fe(III) and Mn(III) complexes are efficient and selective catalysts for countless oxidation reactions.[21−29] Although metalloporphyrins are effective in homogeneous systems, particularly for hydrocarbon epoxidation and hydroxylation, some problems have frequently arisen. For example, secondary reactions deactivate the catalytic species, often leading to low catalytic efficiency. In addition, depending on the structure of the porphyrin ligand, the metalloporphyrin undergoes irreversible destruction. To minimize such issues, scientists have invested considerable effort in the synthesis of porphyrins and metalloporphyrins with more robust structures.[10,25,27,30,31]

The biological significance of copper has long been recognized. However, only in recent decades have a considerable number of research groups turned their attention to the development of synthetic and copper-based functional models of biological systems, which are crucial for the maintenance of life.[32]

Proteins containing copper as the active center usually act as redox catalysts in many biological processes, in electron transfer, or in the oxidation of a large range of organic substrates.[33] In general, copper proteins have four main functions: absorption, storage, and transportation of metal

Received: January 26, 2015

DOI: 10.1021/acs.inorgchem.5b00196
Inorg. Chem. XXXX, XXX, XXX−XXX

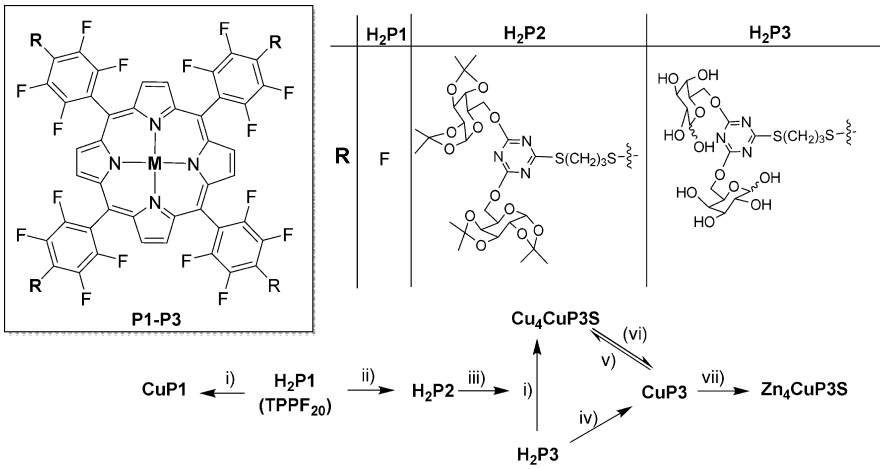

Figure 1. Schematic representation of the reactions of porphyrin H_2TPPF_{20} (**H_2P1**) with the sugar dendrimer GalProt, to obtain the tetrasubstituted galactodendritic conjugates **H_2P2** and **H_2P3**, the corresponding copper(II) complexes **CuP1** and **CuP3**, and the coordination polymers **Cu_4CuP3S** and **Zn_4CuP3S**.

ions; absorption, storage, and transportation of oxygen; electron transfer; and catalysis.[33,34] For instance, hemocyanin underlies oxygen transport in some mollusks and arthropods, whereas tyrosinase and catechol oxidase catalyze the oxidation of phenolic substrates into catechols (tyrosinase) and then to quinones (tyrosinase and catechol oxidase). The latter undergo polymerization to produce the pigment melanin.[35]

As far as catechol oxidation by copper complexes is concerned, research teams have studied several mononuclear and dinuclear copper complexes and investigated their reactivity toward oxygen.[32] These copper compounds have functioned as biomimetic models of the active site of copper proteins; their activity resulted from their structural features. Evaluation of the catecholase activity of copper complexes, for example, the use of 3,5-di-*tert*-butylcatechol as substrate, has helped to identify functional models of metalloenzymes or new catalysts for oxidation reactions.[36]

Following our interest in the development of efficient catalysts that are easy to recover and reuse,[28,30,31] the present work reports on the synthesis and characterization of the new copper porphyrin **CuP3** (Figure 1) and shows that it acts as an efficient catalyst in heterogeneous medium. The use of excess copper(II) acetate (5 equiv) during complexation of the corresponding free-base **H_2P3** or treatment of the copper complex **CuP3** with excess copper(II) acetate (4 equiv) afforded the insoluble solid **Cu_4CuP3S** in the presence of dendrimer groups in the fluorinated porphyrin core. The new material **Zn_4CuP3S**, obtained by treating **CuP3** with zinc(II) acetate, confirmed the coordination ability of the dendrimer units. We compared the catalytic activity of the synthesized solids with the catalytic activity of the soluble copper complexes **CuP3** and **CuP1** during (*Z*)-cyclooctene oxidation by iodosylbenzene. We also assessed the performance of the solid catalyst that gave the best results, **Cu_4CuP3S**, in the epoxidation and hydroxylation of other organic substrates by iodosylbenzene or hydrogen peroxide (e.g., catechol oxidation).

2. EXPERIMENTAL SECTION

2.1. General. ^{1}H and ^{19}F NMR spectra were recorded on a Bruker Avance 300 spectrometer at 300.13 and 282.38 MHz, respectively. Deuterated dimethyl sulfoxide and deuterated chloroform were used as solvents, and tetramethylsilane (δ = 0 ppm) was employed as the internal standard. Chemical shifts are reported in ppm (δ), and coupling constants (J) are given in Hz. Mass spectra were acquired on a 4800 Proteomics Analyzer mass spectrometer (MALDI TOF/TOF). Electronic spectra (UV−vis) were obtained on a Cary-Varian spectrophotometer, in the 300−800 nm range. For solid samples, spectra were recorded in a quartz cell (Hellma) with 0.1 cm path length in mineral oil. Transmission Fourier transform infrared (FTIR) spectra were registered on a Biorad 3500 GX spectrophotometer in the 400−4000 cm^{-1} range, using KBr pellets. KBr was ground with a small amount of the solid to be analyzed, and the spectra were collected with a resolution of 4 cm^{-1} and accumulation of 32 scans. Electron paramagnetic resonance (EPR) measurements of the powder materials were accomplished on an EPR Bruker EMX microX spectrometer (frequency X, band 9.5 GHz) at room temperature and 77 K (using liquid N_2), in the perpendicular microwave polarization X-band.

The products from the catalytic oxidation reactions were quantified on a gas chromatograph Agilent 6850 (FID detector) equipped with a capillary column DB-WAX (J&W Scientific). Quantitative analysis was based on the internal standard method.

All the chemicals used in this study were purchased from Aldrich, Sigma, or Merck and were of analytical grade. Iodosylbenzene (PhIO) was synthesized by hydrolysis of iodosylbenzene diacetate.[37] The obtained solid was dried under reduced pressure and kept at 5 °C; its purity was determined by iodometric titration.

2.2. Synthesis of Copper Porphyrins CuP1 and CuP3. The free-base porphyrins **H_2P1** and **H_2P3** were synthesized as previously described in the literature[38,39] (see Supporting Information). The metalloporphyrins **CuP1** and **CuP3** (Figure 1) were obtained from **H_2P1** and **H_2P3**, respectively, by means of the modified Kobayashi method.[40] Briefly, the metalation reactions were performed with copper(II) acetate in dimethylformamide (DMF); excess copper salt was used to obtain **CuP1**, and a **H_2P3**/copper(II) acetate stoichiometric ratio of 1:1 was employed to synthesize **CuP3**. The reactions were conducted at 120 °C for 3 and 24 h in the cases of **H_2P1** and **H_2P3**, respectively, under magnetic stirring. The solvent was removed under reduced pressure. **CuP1** was washed with water to remove excess salt and purified by column chromatography using dichloromethane as eluent. **CuP3** was washed with a water/acetone mixture (1:1; v/v), to remove any remaining free-base porphyrin, and was successively washed with water and warm methanol. The resulting washing solutions were analyzed by UV−vis spectroscopy, and no free-base porphyrin was detected. The compounds were characterized by UV−vis, FTIR, and EPR spectroscopies. **CuP1** ($C_{44}H_8F_{20}N_4Cu$): UV−vis (DMF) λ_{max}, nm (log ε): 410 (5.31), 536 (3.90), and 570 (3.50). **CuP3** ($C_{116}H_{120}F_{16}N_{16}O_{48}S_8Cu$) UV−vis (DMF) λ_{max}, nm (log ε): 414 (5.19), 538 (3.88), and 572 (3.38). **CuP3 MS**: calcd. for $C_{116}H_{121}F_{16}N_{16}O_{48}S_8Cu$ [M + H]$^+$ 3129.4 found 3129.3; calcd for $C_{116}H_{120}F_{16}N_{16}O_{48}S_8CuNa$ [M + Na]$^+$ 3151.4, found 3151.3.

DOI: 10.1021/acs.inorgchem.5b00196
Inorg. Chem. XXXX, XXX, XXX−XXX

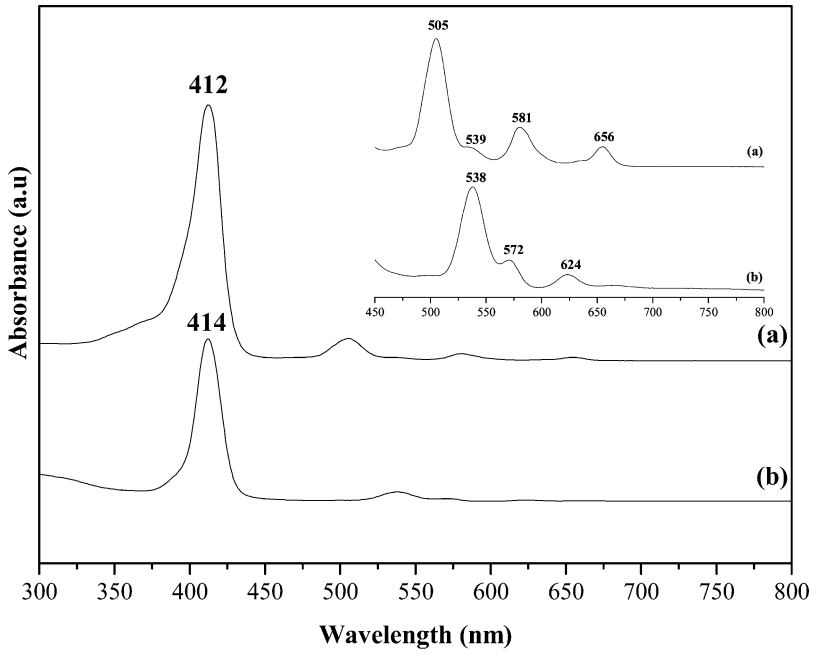

Figure 2. UV−vis spectra of (a) H_2P3 and (b) CuP3 obtained in DMF after the first 15 min of metalation.

2.3. Synthesis of the Porphyrinic Materials Cu_4CuP3S and Zn_4CuP3S. The insoluble purple solid **Cu_4CuP3S** (this abbreviation is related with the number of copper(II) acetate equivalents used during its preparation) was prepared under magnetic stirring at 120 °C by reacting compounds **H_2P3** and **CuP3** with 5 and 4 equiv of copper(II) acetate in DMF for 3 and 24 h, respectively (Figure 1). The insoluble purple solid **Zn_4CuP3S** (this abbreviation is related with the number of zinc(II) acetate equivalents used during its preparation) was prepared by reacting **CuP3** with 4 equiv of zinc(II) acetate salts in the previous conditions. The solids **Cu_4CuP3S** and **Zn_4CuP3S** precipitated at the end of the reactions. **Cu_4CuP3S** and **Zn_4CuP3S** were then washed with different solvents (DMF, tetrahydrofuran, H_2O, and acetone), to remove any remaining free-base porphyrin **H_2P3** and copper(II) or zinc(II) acetates. Subsequently, **Cu_4CuP3S** and **Zn_4CuP3S** were dried in air, at room temperature, and characterized by different techniques.

Treatment of the insoluble solids **Cu_4CuP3S** and **Zn_4CuP3S** with an acidic solution (HCl, 4 mol/L) afforded the soluble metalloporphyrin **CuP3**. UV−vis and EPR spectroscopies confirmed that this sample was identical to the sample that originated from metalation of **H_2P3** with 1 equiv of copper(II) acetate.

2.4. Study of the Catalytic Activity of the Copper Porphyrins CuP1, CuP3, Cu_4CuP3S, and Zn_4CuCuP3S. *2.4.1. Oxidation of Cyclooctene, Cyclohexene, Cyclohexane, and Cyclohexanol.* The efficiency of **CuP3**, **Cu_4CuP3S**, **Zn_4CuP3S**, and **CuP1** (for comparison) as catalysts in oxidation reactions was tested; (*Z*)-cyclooctene and iodosylbenzene were used as substrate and oxidant, respectively. The activity of the best catalyst for (*Z*)-cyclooctene oxidation, **Cu_4CuP3S**, was also evaluated in the oxidation of cyclohexene (previously purified on alumina column), cyclohexane, and cyclohexanol; iodosylbenzene was employed as oxidant. The reactions were performed in a 2 mL thermostatic glass reactor equipped with a magnetic stirrer, in a dark chamber. The catalyst **CuP*x*** and the oxidant iodosylbenzene (**CuP*x*/**PhIO at a molar ratio of 1:50) were purged with argon for 15 min and then suspended in 400 μL of acetonitrile. Next, the substrate was added at a **CuP*x*/**PhIO/substrate molar ratio of 1:50:5000. The 1:50 catalyst/oxidant molar ratio was based on the molecular mass of the metalloporphyrin, including the insoluble solid catalysts **Cu_4CuP3S** and **Zn_4CuP3S**. The oxidation reactions were performed under magnetic stirring for the required time (1 or 3 h). At the end of the reaction, excess iodosylbenzene was eliminated by addition of sodium sulfite. The catalysts **Cu_4CuP3S** and **Zn_4CuP3S** remained insoluble during all the reaction, so the process was heterogeneous in these cases. At the end of the heterogeneous reactions, the reaction mixture was separated from the insoluble catalyst by centrifugation and transferred to a volumetric flask. The solid catalyst was washed several times with methanol and acetonitrile, to extract any reaction products that might have adsorbed onto the solid catalyst. The washing solutions were added to the previously separated reaction supernatant. The products present in the resulting solution were analyzed by gas chromatography; 1-octanol was the internal standard. Product yields were based on the quantity of PhIO added to each reaction. Control reactions were also performed in the absence of metalloporphyrin; the aforementioned methodology was used.

To study the recyclability of the solid **Cu_4CuP3S**, the solid catalyst recovered after the first use was washed with different solvents (water, methanol, acetonitrile, and dichloromethane) and dried at 55 °C for 48 h. The dried solid was then reused in a new catalytic reaction in the same conditions as the ones described above. To evaluate whether the investigated solid metalloporphyrins solubilized during the washing process, the resulting washing solutions were analyzed by UV−vis spectroscopy. Application of the Sheldon test to the catalytic system helped to verify the real heterogeneous character of the process involving the catalyst **Cu_4CuP3S**.[41] To this end, the catalyst was removed from the reaction solution by centrifugation after 15 min of reaction. More oxidant was added to the reaction solution, and the product contents were monitored after another 15 min of reaction.

2.4.2. Oxidation of Catechol. The catalytic efficiency of **Cu_4CuP3S** and **CuP1** (for comparison) was also investigated during catechol oxidation. Hydrogen peroxide was used as oxidant. In a typical reaction, the solid catalyst and the substrate (catechol) were placed in a 10 mL volumetric flask. Then, 7.1 mL of phosphate buffer (pH = 8.0) and 10 μL of hydrogen peroxide (30% solution v/v) were added to the flask. The volume was completed with deionized water. The **CuP*x*/**H_2O_2/catechol molar ratio was 1:1000:100. When hydrogen peroxide was used as oxygen donor it was necessary to use a higher molar ratio to compensate for the dismutation side reaction frequently observed with this compound. The reaction was performed in the dark, for reaction times ranging from 15 min to 2 h, under constant stirring. A thermostatic bath (30 °C) was employed. The progress of the catalytic reaction was monitored by UV−vis spectroscopy (band at 508 nm, ε = 13.536 L mol^{-1} cm^{-1}), and the reaction products were quantified with the aid of the nitrite method.[42] The catalytic reaction was also monitored from a kinetic viewpoint. To this end, aliquots

DOI: 10.1021/acs.inorgchem.5b00196
Inorg. Chem. XXXX, XXX, XXX−XXX

were withdrawn from the reaction mixture every 15 min and analyzed by the same nitrite method.[42] After the first use, the catalyst **Cu_4CuP3S** was recovered from the reaction medium, washed with water, dried at 50 °C, and reused in another catalytic reaction cycle where catechol was the substrate. The resulting washing solution was recovered and analyzed by UV−vis spectroscopy to verify whether any **CuP3** was lost during the washing process.

3. RESULTS AND DISCUSSION

3.1. Characterization. *Solution and Solid-State UV−visible Spectroscopy.* By recording the electronic spectra at different reaction times, it was possible to follow the metalation of the free-base porphyrins **H_2P1** (Supporting Information, Figure S1) and **H_2P3** (Figure 2).

The UV−vis spectrum of **CuP1** (not shown) presented the characteristic Soret band at 414 nm, which was slightly red-shifted as compared with the Soret band of the corresponding free-base porphyrin **H_2P1** (412 nm). The spectrum of **CuP1** also displayed two Q-bands, at 536 and 570 nm, because the microsymmetry of the porphyrin macrocycle changed from D_{2h} in **H_2P1** to D_{4h} in **CuP1** after introduction of copper(II) into the porphyrin core (Supporting Information, Figure S1).[43]

The UV−vis spectrum obtained after metalation of **H_2P3** with 1 equiv of copper(II) acetate also differed from the UV−vis spectrum of the corresponding free-base porphyrin. This confirmed that the metalation reaction introduced copper(II) into the inner core of **H_2P3**. The characteristic Soret band of the metalloporphyrin appeared at 414 nm, whereas the three Q-bands arose at 538, 572, and 624 nm. All these bands were due to the complex **CuP3**. Indeed, washing of **CuP3** with a water/acetone mixture at the end of the synthesis must have completely solubilized and removed the free-base porphyrin. Interestingly, metalation of the free-base **H_2P3** in the presence of excess copper(II) acetate elicited alterations in the free-base Q-band profile of the UV−vis spectrum within the first 15 min of reaction. This was possible to follow because some copper porphyrin solubilized in DMF (Figure 2). At the end of the reaction, a solid designated **Cu_4CuP3S** precipitated. This solid was very little soluble in solvents where **H_2P3**, **H_2P1**, and **CuP1** were soluble or partially soluble (e.g., toluene, methanol, chloroform, dichloromethane, acetone, ethanol, acetonitrile, dimethylformamide, tetrahydrofuran, and water). The marked insolubility of **Cu_4CuP3S** in conventional solvents suggested that, after metalation of the inner core of the **H_2P3** macrocycle, the excess metal used in the reaction interacted with the galactose units in the porphyrin ring, to afford a robust and insoluble coordination polymer.

The UV−vis spectrum of solid **Cu_4CuP3S** obtained in mineral oil after the purification process (Figure 3) displayed a broad Soret band at 420 nm, which was slightly red-shifted as compared with the Soret band of **H_2P3** (412 nm). The alteration in the number and position of Q bands confirmed that the metalation process occurred.

According to the literature, a porphyrin ring bearing dendrimer groups in the periphery of the macrocycle affords supramolecular structures via self-assembly.[44] These structures present low solubility in the solvent used for their synthesis as well as in other tested solvents. In another work, the coordination of the metal ion by phosphoryl substituents justified the formation of a two-dimensional (2D) structured solid based on a copper porphyrin containing phosphoryl substituents in the macrocycle.[45] Hence, although for copper(II) the four-coordination is usually expected, literature survey

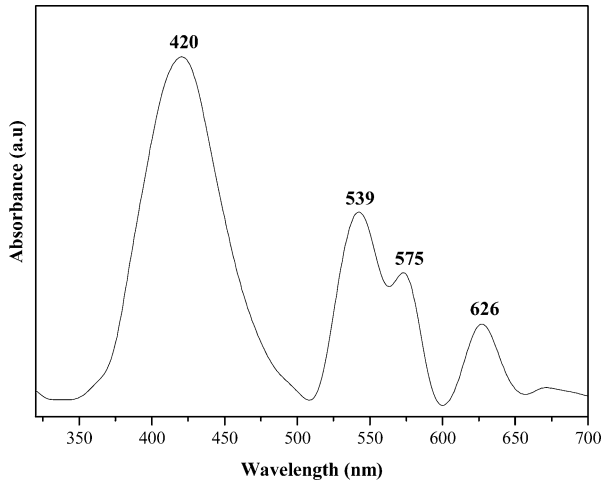

Figure 3. UV−vis spectrum of solid **Cu_4CuP3S** dispersed in mineral oil.

confirms that depending on the porphyrin substituents, other coordination modes can be observed and are responsible by the design of new solids.[45] Knowing that dendrimers favor the formation of supramolecular structures,[44] in this study the coordination of the dendrimers substituents with external copper ions can be responsable for the formation of the 2D structures.

Furthermore, metalloporphyrins with appropriate substituents on the periphery of the porphyrin ring constitute efficient building blocks for the design and synthesis of coordination polymers (CPs).[46,47] CPs[47−50] originate from the binding between an organic or inorganic linker and metallic centers by self-assembly, to give usually robust and nanoporous mono-, bi-, or tridimensional supramolecular structures.[49] CPs are insoluble, and their preparation must occur by self-assembly in a single step.[48]

Depending on the coordination tendencies and geometries of the substituents in the porphyrin macrocycle, porphyrin-based supramolecular systems can establish different interactions. For example, porphyrin macrocycles can interconnect via a ligand group (van der Waals bonding). Alternatively, one donor atom present in the substituent in the periphery of the metalloporphyrin ring can coordinate with the metal center of another metalloporphyrin.[47,51]

When the substituents in the porphyrin core bear carboxyl or pyridyl groups, they may favor the formation of CPs with different metal centers (Fe, Co, and Zn, among others), because carboxyl and pyridyl can act as a linker.[51]

Here, the fact that solid **Cu_4CuP3** emerged during metalation of **H_2P3** with excess copper salt might be related with the ability of galactose dendrimer units to form a structured solid, like a CP, by self-assembly mediated by the copper ions.

To evaluate the ability of the galactose dendrimeric substituents in **H_2P3** to act as linkers and afford insoluble and structured solids, we designed two additional experiments. One of the experiments involved reaction of the soluble porphyrin **CuP3**, obtained from the metalation process that used 1 equiv of copper(II) acetate, with excess copper(II) acetate (4 equiv) in DMF. This experiment provided a solid with features (vide infra) that resembled the features of solid **Cu_4CuP3S** obtained directly from treatment of free-base **H_2P3** with excess copper(II) salt. The other experiment involved

DOI: 10.1021/acs.inorgchem.5b00196
Inorg. Chem. XXXX, XXX, XXX−XXX

reaction of **CuP3** with excess zinc(II) acetate at a 1:4 molar ratio in DMF, which furnished a solid designated **Zn_4CuP3S**.

The UV−vis spectrum of **Zn_4CuP3S** dispersed in mineral oil maintained the characteristic profile bands of **CuP3** (Supporting Information, Figure S2).

Compounds **Cu_4CuP3S** and **Zn_4CuP3S** were soluble under acidic conditions (HCl 4.0 mol/L). The residue generated after treatment of these solids with acid, drying, and analysis by mass spectrometry (MALDI TOF/TOF) exhibited the same characteristics as **CuP3**. Therefore, **Cu_4CuP3S** and **Zn_4CuP3S** have a somewhat organized structure mediated by metal ions, but interaction of these solids with protons breaks this structure and gives the monomeric **CuP3.**

Fourier Transform Infrared Analysis. The FTIR spectra of the free-base porphyrins **H_2P1** and **H_2P3** exhibited the typical bands of this class of ligands[52] (Figure 4). The bands at 1600

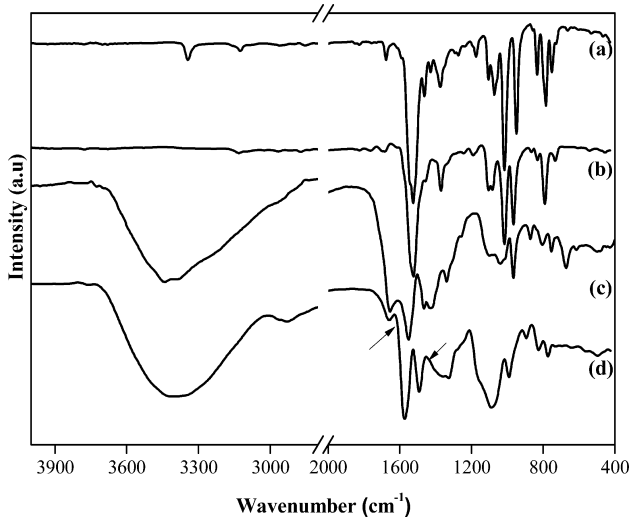

Figure 4. FTIR spectra of the free-base porphyrins and copper porphyrins: (a) Porphyrin **H_2P1**, (b) **CuP1**, (c) Porphyrin **H_2P3**, and (d) **Cu_4CuP3S**.

cm^{-1} corresponded to symmetric angular deformation in the N−H plane of the pyrrole ring; the bands at 3313, 3116, and 2937 cm^{-1} referred to NH, CH (phenyl), and CH (pyrrole) stretching. The bands relative to in-plane δ N−H and out-of-plane δ N−H appeared at 970 and 752 cm^{-1}, respectively, among other bands related with skeletal ring vibrations. In the spectrum of **H_2P3**, the bands at 3442 cm^{-1} (stretching OH) and 672 cm^{-1} (stretching C−N) were due to the glycodendritic moieties.

Complex **CuP1** displayed the characteristic bands of porphyrin **H_2P1**. Only the bands in the region of 3000 cm^{-1}, relative to symmetric and asymmetric NH stretching, and in the region of 1600 cm^{-1}, related to another vibrational mode, were absent. The spectrum of solid **Cu_4CuP3S** resembled the spectrum of porphyrin **H_2P3**. A strong band emerged near 1000 cm^{-1}, due to the metalloporphyrin skeletal ring,[52,53] in agreement with literature results.[54]

The absence of bands typical of acetate ions (bands in the region of 1610 and 1420 cm^{-1},[54] attributed to symmetric and asymmetric stretching of C═O species, and indicated by the arrows in Figure 4d) suggested that the washing process successfully removed this anion and prevented its coordination to the metal.

Electron Paramagnetic Resonance Analyses. Figures 5 and 6 illustrate the EPR spectra of the prepared compounds. EPR is

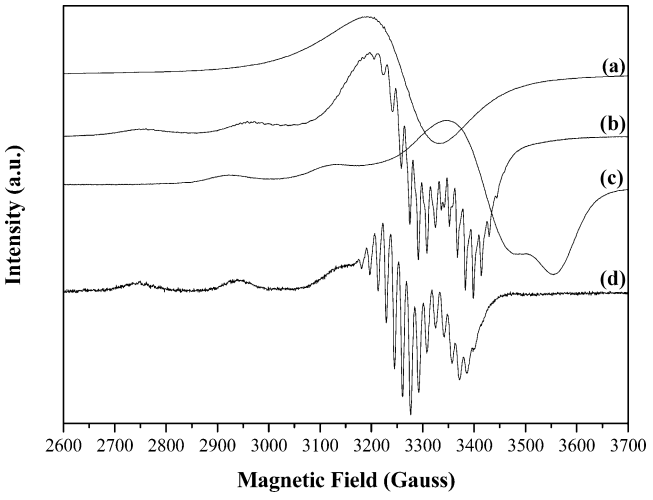

Figure 5. EPR spectra of copper porphyrins at 77 K: (a) **CuP1** as solid, (b) **CuP1** in dichloromethane solution, (c) **CuP3** as solid, and (d) **CuP3** in dimethylformamide solution.

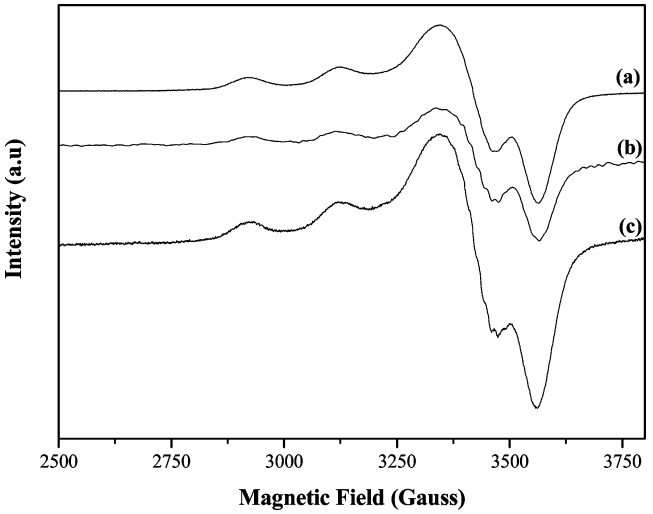

Figure 6. EPR spectra of copper materials at 77 K: (a) **Cu_4CuP3S** (solid sample), (b) **Cu_4CuP3S** obtained by overnight reaction of **CuP3** with $Cu(OAc)_2$ (1:4) (solid sample), and (c) **Zn_4CuP3S** (solid sample).

a valuable tool to investigate copper complexes, because the copper(II) ion presents a d^9 electronic configuration and one unpaired electron. The EPR spectrum of copper(II) can provide relevant information regarding the oxidation state, binding mode, and symmetry of a copper compound.[55−62] The copper atom (^{63}Cu or ^{65}Cu) has nuclear spin of $I = 3/2$, which causes hyperfine splitting between the unpaired electron and the nucleus itself. As a consequence, the EPR spectrum of copper(II) consists of four wide lines. For many compounds where the d electrons are delocalized to a considerable extension over the ligands (which may have nuclear spin other than zero), superhyperfine splitting may superimpose on these lines.[54] Copper(II) centers typically have tetrahedral geometry or octahedral geometry elongated along the *z*

DOI: 10.1021/acs.inorgchem.5b00196
Inorg. Chem. XXXX, XXX, XXX−XXX

direction. Their spectra are anisotropic and usually show signs of axial or orthorhombic symmetry.

The EPR spectrum of a solid sample of **CuP1** (Figure 5a) exhibited a single EPR signal with isotropic character and did not present hyperfine lines,[56] as expected for copper(II) species. On the other hand, the EPR spectrum of **CuP1** in dichloromethane solution at 77 K (Figure 5b) displayed the characteristic anisotropic signal expected for copper(II) with axial symmetry ($g_{//} > g_{\perp}$) and hyperfine splitting ($A_{//} \approx 195$ G).

Figure 5b also evidenced a multiple-line pattern in the perpendicular spectrum region. This is typical of superhyperfine interaction of the copper(II) ion unpaired electron with the four magnetically equivalent ^{14}N nucleus ($I = 1$), which should result in the expected deployment of each signal in nine lines.[57]

The EPR spectrum of **CuP3** (solid sample, Figure 5c) showed the characteristic anisotropic signal of copper(II), $S = 3/2$, in axial symmetry in the region of $g = 2.0$. The values of $g_{//}$ differed from the values of $g_{\perp}$, and the four EPR lines expected for copper(II) species emerged. The EPR spectrum of **CuP3** in DMF solution at 77 K (Figure 5d) provided better resolution of the typical hyperfine and superhyperfine lines due to interaction of copper(II) with the four nitrogen atoms of the coordinative ligands.

The EPR spectra of many pure solid copper(II) complexes exhibit the signal relative to hyperfine splitting. However, the signal due to superhyperfine splitting originating from interaction between the unpaired copper(II) electron and the ligand with nuclear spin values (I) different from zero does not appear.[58]

The EPR spectra of solids **Cu$_4$CuP3S** and **Zn$_4$CuP3S** displayed an anisotropic signal with the four characteristic lines of copper(II), axial symmetry in the region of $g = 2.0$, and different values of $g_{//}$ and $g_{\perp}$ (Figure 6).

Table 1 lists the EPR parameters (g values and A constant) obtained by simulating the experimental spectrum of complexes

Table 1. Spin Hamiltonian Parameters Obtained for the X-band EPR Spectral Simulations[a] of CuP1, CuP3, Cu$_4$CuP3S, and Zn$_4$CuP3S at 77 K

compound	$A_{//Cu}$[b]	$g_{//}$	$A_{\perp Cu}$[b]	$g_{\perp}$	A_N[b]	α^2
CuP1	210	2.189	28	2.054	17.2	0.834
CuP3	190	2.208	26	2.040	18	0.789
Cu$_4$CuP3S[c]	198	2.185	20	2.049	18	0.792
Cu$_4$CuP3S[d]	198	2.185	20	2.049	18	0.792
Zn$_4$CuP3S	200	2.185	24	2.047	18	0.797

[a]The EPR parameters listed above were obtained by simulating the experimental spectrum for **CuP1** in dichloromethane solution, **CuP3** in dimethylformamide solution, and the solid samples **Cu$_4$CuP3S** and **Zn$_4$CuP3S** at 77 K. The Simfonia simulation pack software was employed. [b]Hyperfine coupling constants in units of 10^{-4} cm^{-1}. [c]Solid **Cu$_4$CuP3S** was prepared by reacting the free-base **H$_2$P3** with Cu(OAc)$_2$ (molar ratio 1:5; see Experimental Section). [d]Solid **Cu$_4$CuP3S** was prepared by reacting **CuP3** with Cu(OAc)$_2$ (molar ratio 1:4) overnight.

CuP1, **CuP3**, solid **Cu$_4$CuP3S**, and solid **Zn$_4$CuP3S** with the aid of the Bruker WinEPR SimFonia software.[58] The A_N value (superhyperfine interaction constant = 18 G) simulated for compound **CuP3** indicated that (i) the copper(II) ion coordinated to the nitrogen atoms, (ii) the orbitals overlapped well, and (iii) the configuration was planar. A_N values lay between 17 and 18 G, in accordance with values frequently found for copper porphyrins.[58] For compounds **CuP1** and **CuP3**, $g_{//}$ was higher than $g_{\perp}$, and both were larger than 2.0 (Table 1) in all the recorded EPR spectra. Therefore, in both complexes the unpaired d electron occupied the $d_{x^2-y^2}$ copper d orbital in the equatorial plane of copper(II) with elongated tetragonal symmetry.[58,59]

The g-tensor values for the simulated spectra of **CuP1** and **CuP3** were $g_{//} = 2.18$, $g_{\perp} = 2.03$ and $g_{//} = 2.21$, $g_{\perp} = 2.04$, respectively. These values agreed with values found for metalloporphyrins with D_{4h} symmetry (square planar) around the copper(II) ion.[60]

Nonomura et al.[58] studied copper(II) complexes of porphyrins, chlorins, and phthalocyanines and demonstrated a strict relationship between the values of $A_{//}$, $g_{//}$, and the degree of distortion in these compounds; that is, a larger distortion was associated with greater $g_{//}$ and lower $A_{//}$ values.

Comparison of the values of g-tensor and A measured for **CuP1** and **CuP3** revealed lower values for **CuP3**. The nature of the meso-aryl substituents significantly affected these parameters. **CuP3** was slightly distorted, as characterized by the lowest value of the Cu hyperfine constant $A_{//}$, a result of the existence of bulky ligands in the **H$_2$P3** porphyrin ring.

The parameter covalency factor (α^2) describes the in-plane metal−ligand σ bonding;[62,63] it provides information about how ligands disturb the electronic levels of the central metal ion. The value of α^2 is equal to and lower than 1 for systems that present pure ionic bonding and covalent bonding, respectively. Application of the experimental EPR parameters in the Kivelson and Neiman equation,[64] $\alpha^2 = [A_{//}/P + (g_{//} - 2.0023) + 3/7(g_{\perp} - 2.0023) + 0.04]$ (where P is the spin−orbit coupling factor), gives the α^2 values. The metal ions in the metalloporphyrins are sensitive to the molecular environment around them; hence, α^2 changes as a function of the ligand. Using $P = 0.036$ cm^{-1}[58,60] and the values of $g_{\perp}$, $g_{//}$, and $A_{//}$ given in Table 1, it was possible to calculate α^2 values for **CuP1** and **CuP3** 0.834 and 0.799, respectively, which were consistent with the values of α^2 obtained for copper(II) porphyrins and other copper complexes.[60,61] These values provided a qualitative idea of the σ-covalency of the Cu−N bonds in the studied metalloporphyrins and showed that the mesosubstituents in porphyrin **H$_2$P3** affected the nature of the M−N bonding. Since **CuP3** had lower α^2 than **CuP1**, there was more σ-covalency between copper and nitrogen in the case of **CuP3**.

Comparison of the values of tensor g and constant A simulated for the two solids **Cu$_4$CuP3S** prepared herein ($g_{//} = 2.185$ and $A_{//} = 184$ G, regardless of the preparation method) with the parameters obtained for complexes **CuP1** ($g_{//} = 2.189$ and $A_{//} = 195$ G) and **CuP3** ($g_{//} = 2.208$ and $A_{//} = 177$ G) indicated the presence of **CuP3** in solid **Cu$_4$CuP3S** and the presence of copper atom linking the metalloporphyrins. It is noteworthy that both solids **Cu$_4$CuP3S** (synthesized directly from **H$_2$P3** or via **CuP3**) afforded the same EPR parameters, so both synthetic strategies must have led to the same solid.

Figure 6 and Table 1 present the characterization of solid **Zn$_4$CuP3S** by EPR as well as the parameters obtained by simulating the experimental spectrum. The values of $g_{\perp}$, $g_{//}$, and $A_{//}$ for **Zn$_4$CuP3S** and **CuP3** were similar (Table 1), showing that the presence of zinc(II) ions acting as linker did not affect the metalloporphyrinic core. Furthermore, the values of α^2 calculated for the materials containing **CuP3**, that is, **Cu$_4$CuP3S** and **Zn$_4$CuP3S**, were similar to the values of α^2 obtained for free **CuP3**.

DOI: 10.1021/acs.inorgchem.5b00196
Inorg. Chem. XXXX, XXX, XXX−XXX

3.2. Investigation of the Catalytic Activity. This work tested the catalytic efficiency of the highly insoluble solids **Cu_4CuP3S** and **Zn_4CuP3S** in (*Z*)-cyclooctene oxidation under heterogeneous conditions and compared it with the catalytic activity of **CuP1** and **CuP3** under homogeneous conditions. It also investigated the catalytic efficiency of **Cu_4CuP3S** in the biomimetic oxidation of cyclohexene, cyclohexane, cyclohexanol, and catechol.

3.2.1. Oxidation of Different Organic Substrates Using Iodosylbenzene as Oxidant. Since the 1970s, the scientific literature has brought countless reports on the use of iron and manganese porphyrins as catalysts for oxidation reactions.[65−77] Considering the efficiency of copper(II) porphyrins and analogues in oxidative processes, Keilin found in the 1950s that the supposed catalytic activity of a natural Cu(II) porphyrin on the O_2-oxidation of ascorbic acid and cysteine is due to extraneous Cu and not to the Cu(II) present in porphyrin core,[78] as it was mentioned in previous research.[79] However, other work published since then has confirmed that some copper(II) complexes of porphyrins or analogues are able to act as efficient catalysts in the oxidation of different substrates using O_2 or peroxides as oxidants.[80−87] In these works the main agent responsible for the catalytic activity was considered copper(II) macrocycle, but no mechanistic proposal was discussed.

(*Z*)-Cyclooctene is an excellent substrate model to evaluate the catalytic efficiency of novel metalloporphyrins: it is easy to oxidize, and (*Z*)-cyclooctene oxide is generally the sole product.[88]

Metalloporphyrins bearing bulky and/or electronegative ligands at the ortho positions of the meso substituents of the porphyrin core are efficient and selective catalysts for oxidation reactions.[67,68] The substituents in the porphyrin periphery can help to generate and stabilize the active catalytic species, thereby avoiding porphyrin destruction by self-interaction in solution.[67] Porphyrin **H_2P1** is an example of this kind of ligand, and the corresponding manganese and iron complexes afford good catalytic oxidation results.[67,68] As for **CuP3** prepared herein, on the one hand it presents bulkier substituents than **CuP1**. On the other hand, substitution of one fluorine atom per meso-phenyl substituent in the porphyrin ring with the dendrimer removes some of the electron-withdrawing groups that contribute to stabilization of the active catalytic species.[25,30,67,69]

Table 2 shows that **CuP1** was a good catalyst for (*Z*)-cyclooctene epoxidation. The epoxide yield was 80% (Table 2, run 1), in agreement with the similar yields reported for iron(III) and manganese(III) porphyrins in the literature,[31,68,69,89] although this direct comparison in terms of intermediate species is not possible. Fe and Mn porphyrins catalyze oxidation reactions via high-valent metal-oxo or hydroperoxy species. On the basis of electrochemical studies involving simple Cu porphyrin systems, first and second oxidation reactions are ligand-centered, yielding π-cation species;[82] other studies show that hydroperoxy species are also possible intermediates.[84] However, there is not yet strong evidence to propose a real intermediate for copper(II) porphyrin mediated oxidation reactions.

However, the data in Table 2 showed that introduction of the dendritic units diminished the catalytic efficiency of the homogeneous catalyst **CuP3** (45% vs 80% epoxide yield for **CuP1**), which contrasted with the results achieved for solid **Cu_4CuP3S**. In fact, the excellent catalytic activity of **Cu_4CuP3S**

Table 2. Epoxide Obtained during (*Z*)-Cyclooctene Oxidation by Iodosylbenzene in the Presence of Different Solid Catalysts[a]

catalyst[a]	run	(*Z*)-cyclooctene epoxide yield[b] (%)
CuP1	1	80 ± 2.0
CuP3	2	45 ± 2.0
Zn_4CuP3S	3	40 ± 1.3
Cu_4CuP3S[c]	4	90 ± 1.0
first reuse[c]	5	84 ± 1.2
second reuse[c]	6	82 ± 1.0
third reuse[c]	7	80 ± 2.0
fourth reuse[c]	8	81 ± 1.2
Cu_4CuP3S[d]	9	91 ± 1.7
$Cu(AcO)_2$ + PhIO	10	15 ± 1.0
control	11	12 ± 1.2

[a]Reaction conditions: reaction time = 1 h, **CuP*x***/PhIO/substrate molar ratio = 1:50:5000. All the reactions were performed at least in duplicate. [b]The product yields were calculated on the basis of the amount of iodosylbenzene used in the reaction. [c]The **Cu_4CuP3S** catalyst was recovered for use in a new catalytic reaction by centrifugation of the reaction solution, followed by washing and drying of the solid, as explained in the experimental section. [d]solid **Cu4CuP3S** was prepared by reacting the metalated **CuP3** and $Cu(OAc)_2$ (1:4) overnight.

(90% epoxide yield) as compared with **CuP3** suggested that coordination of **CuP3** with four extra copper(II) ions generated a much more organized/active solid system. The cavity that emerged in this system was able to retain the reagents and increase their exposure to the metal center (porphyrin core or/and Cu(II) bound dendrimers units), thereby improving the reaction rate and the product yield.

The catalytic activity of solid **Zn_4CuP3S** (Table 2, run 3, 40% epoxide yield) resembled the activity of **CuP3** (Table 2, run 2, 45% epoxide yield). Hence, **CuP3** and the solid obtained by coordination of **CuP3** with four zinc(II) ions (**Zn_4CuP3S**) furnished similar active catalytic species, suggesting that the zinc(II) ion only served to stabilize the structure of **Zn_4CuP3S**, without significantly affecting the catalytic performance. This result corroborated the EPR data, which had evidenced the presence of copper porphyrin in solid **Zn_4CuP3S** (Figure 6).

Interestingly, the catalytic activity of solid **Cu_4CuP3S** (90% epoxide, run 4, Table 2) was almost twofold the catalytic activity of solid **Zn_4CuP3S** and slightly better than **CuP1** (80% epoxide, run 1, Table 2). The way the copper porphyrin and the linking groups lay in **Cu_4CuP3S** probably helped to maintain the structure of the solid favoring the catalytic performance, although the degree to which this configuration is important for catalysis is unknown. It is important to point out that Cu(II) bound to dendrimers units can have some role in the catalytic activity of this heterogeneous solid.

The Sheldon test confirmed the real heterogeneous character of the process in the case of catalyst **Cu_4CuP3S**.[41] This test required interruption of the reaction conducted in the presence of **Cu_4CuP3S** after 15 min, to furnish 26% epoxide yield, and catalyst removal from the solution by centrifugation. Addition of more oxidant to the reaction solution that did not contain the solid catalyst any longer and conduction of the reaction for other 15 min did not provide significantly increased epoxide yield (28% vs the previously achieved 26%). Therefore, the removed solid catalyst did account for formation of the oxidation product.

DOI: 10.1021/acs.inorgchem.5b00196
Inorg. Chem. XXXX, XXX, XXX−XXX

Table 3. Products Obtained in the Oxidation of Cyclohexene by Iodosylbenzene Catalyzed by CuP1 and CuP3S[a]

		cyclohexene[b]					
catalyst	run	epoxide[c] (%)	A^c (%)	K^c (%)	total yield (%)	$A + K^d$ (%)	select[e] (%)
CuP1	1	20 ± 1.0	8.0 ± 1.0	33 ± 2.0	61	41	49
Cu_4CuP3S	2	18 ± 1.0	14 ± 1.0	3.2 ± 0.6	35	17	51
control	3	8.0 ± 1.8	1.6 ± 0.4	9.5 ± 1.0	19	11	42

[a]Reaction conditions: reaction time = 1 h, **CuP*x***/PhIO/substrate molar ratio = 1:50:5000. All the reactions were performed at least in duplicate. [b]The product yields were calculated on the basis of the amount of iodosylbenzene used in the reaction. [c]Epoxide = cyclohexene oxide, *A* = cyclohex-2-en-1-ol, and *K*= cyclohex-2-en-1-one. [d]*A* + *K* = alcohol yield + ketone yield. [e]Selectivity for cyclohexene oxide.

Because solid **Cu_4CuP3S** was insoluble in all the catalytic reactions, we decided to investigate its reuse in a second, third, and fourth (*Z*)-cyclooctene epoxidation by iodosylbenzene. The yields of the first, second, third, and fourth reactions were similar (Table 2, runs 5−8), suggesting that the solid catalyst was stable and reusable. UV−vis spectroscopy monitoring of all the reaction solutions and catalyst washing solutions demonstrated that no copper porphyrin leached from solid **Cu_4CuP3S**. Hence, solid **Cu_4CuP3S** did act as a solid catalyst in a heterogeneous process.

The good catalytic performance of **Cu_4CuP3S** prompted us to test its efficiency in the oxidation of cyclohexene (Table 3) and cyclohexane (Table 4).

Table 4. Oxidation of Cyclohexane and Cyclohexanol by Iodosylbenzene Catalyzed by CuP1 and Cu_4CuP3S[a]

	substrate		
	cyclohexane[b]		cyclohexanol[b]
catalyst	cyclohexanol (%)	cyclohexanone (%)	cyclohexanone (%)
CuP1[a]	1.0 ± 0.2		47 ± 2.2
CuP1[c]	1.2 ± 0.2		72 ± 3.3
Cu_4CuP3S[a]	5.1 ± 0.3		23 ± 2.1
Cu_4CuP3S[c]	1.0 ± 0.1	5.0 ± 0.5	83 ± 1.6
control[a,c]			7.7 ± 0.5

[a]Reaction conditions: reaction time = 1 h (a) or 3 h (b), **CuP*x***/PhIO/substrate molar ratio = 1:50:5000. All the reactions were performed at least in duplicate. [b]The product yields were calculated on the basis of the amount of iodosylbenzene used in the reaction. [c]3 h of reaction time.

Cyclohexene oxidation mediated by PhIO/metalloporphyrin (MP) systems are usually yields cyclohexene oxide (major product) and the corresponding allylic products (cyclohex-2-en-1-ol and cyclohex-2-en-1-one).[75,76] These products result from competition between the C=C and the allylic C−H bonds of alkenes for the electrophilic active catalytic species originating from the reaction between the MP and iodosylbenzene.[5,77] However, the allylic products (alcohol and ketone) can also arise via free radical routes mediated by molecular oxygen and not by the intermediate active complex. The reaction conditions (solvent, temperature, inert atmosphere, and reactants molar ratio), the structure of the porphyrin ring,[76] and catalyst arrangement in a support[90] can sometimes control catalyst selectivity.

Cyclohexene oxidation catalyzed by **CuP1** (homogeneous process) and **Cu_4CuP3S** (heterogeneous process) yielded the epoxide (Table 3, runs 1 and 2, respectively); however, allylic products also emerged, suggesting involvement of the radical route.[28,75] Cyclohexene oxide and allylic products also arose in the absence of catalyst, but the epoxide yield was lower (Table 3, control reaction, run 3). Therefore, the copper catalysts participated in epoxide formation.

CuP1 and **Cu_4CuP3S** gave similar epoxide selectivity (49 and 51%, respectively), suggesting that the intermediate species originating from these catalysts were similar. However, allylic products emerged in higher amount in the presence of **CuP1** as compared with **Cu_4CuP3S**, so the total product yield was 61 and 35% for homogeneous and heterogeneous catalysis, respectively. Hence, the epoxide originated from a catalytic route that involved the copper porphyrin, whereas the allylic products resulted from an independent radicalar route.

Table 4 summarizes the results obtained during cyclohexane oxidation catalyzed by **CuP1** and **Cu_4CuP3S**. This substrate enables evaluation of catalytic efficiency and product selectivity, because the reaction can afford cyclohexanol and/or cyclohexanone.

Neither **CuP1** nor **Cu_4CuP3S** was able to produce alcohol efficiently solid **Cu_4CuP3S** gave maximum cyclohexanol yield of 5.0% after 1 h of reaction. Longer reaction times (3 h) did not improve alcohol production, but ketone emerged in the presence of **Cu_4CuP3S**. In this case, the alcohol produced after 1 h of reaction probably underwent catalytic overoxidation to ketone, a process that seemed to be potentiated in the case of **Cu_4CuP3S**. The cavity and pores in this latter catalyst probably favored the permanence of the alcohol near the active site of the solid catalyst and allowed for its reoxidation.

These results prompted us to evaluate the efficiency of these catalysts in cyclohexanol oxidation. According to Table 4, ketone emerged after 1 h of reaction for both catalysts.[31] **Cu_4CuP3S** surpassed the excellent performance of **CuP1** (47 and 72% cyclohexanone yield after 1 and 3 h of reaction, respectively) when the reaction time was 3 h (83% of cyclohexanone yield).

The formation of ketone may also occur via a radical mechanism.[77] Several studies[91,92] have proposed that the catalytic reaction occurs by oxygen transfer from PhIO to the alkanes C−H bonds in a two-step sequence. This mechanism is analogous to the mechanism shown for the allylic oxidation of cyclic alkenes. The first step involves hydrogen atom abstraction from the substrate by a metal-oxo catalytic species, to generate an alkyl radical and hydroxometalloporphyrin in a solvent cage. Recombination (or oxygen rebound) may occur within the cage, to give an alcohol. Additionally, an alkyl radical may escape the cage and react with other species in solution, resulting in several other products.[77]

Again, the structure of solid **Cu_4CuP3S** can justify the better product yield achieved with this catalyst as compared with **CuP1**. Channels and pores in solid **Cu_4CuP3S** may have retained the reactants, and the increment in reaction time may have favored the formation of the active catalyst species, to furnish a greater amount of product.

DOI: 10.1021/acs.inorgchem.5b00196
Inorg. Chem. XXXX, XXX, XXX−XXX

3.2.2. Oxidation of Catechol. In recent years, the oxidation of benzenediols has gained importance because this reaction affords quinones, which display several biological activities such as antitumor,[93] antiprotozoal,[93,94] anti-inflammatory,[95] and leishmanicidal activities[96] and therefore have potential application in the medical field.

Catechol (1,2-benzenediol) oxidation produces *ortho*-benzoquinone, a substance with antimicrobial properties that helps to treat infections in plants.[97] In medicine, catechol oxidation is useful in the area of oncology (cancer-related cells). Some scientific studies[97,98] have claimed that substances originating from catechol oxidation may boost the body's defense against glioblastoma cells, avoiding the formation of malignant tumors.

Researchers have investigated a large number of mono- and binuclear copper complexes as biomimetic models of catecholase enzymes during catechol oxidation.[99,100] Catechol can undergo oxidation and generate the corresponding *ortho*-benzoquinone (Figure 7) through oxidation of the semiquinone

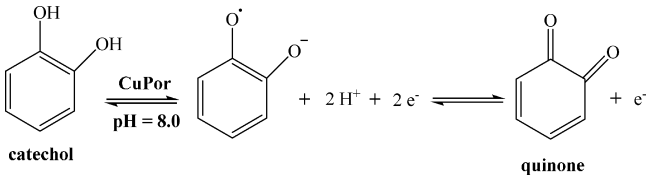

Figure 7. Oxidation of catechol to *ortho*-benzoquinone.

radical intermediate. The resulting quinone may polymerize and give compounds such as melanin.[101] During the catalytic oxidation of catechol molecules, the reaction mixture acquires an intense brown color that later disappears. This brown color indicates that the oxidation reaction is taking place.[100]

We conducted catechol oxidation reactions catalyzed by **CuP1**, **CuP3**, and **Cu_4CuP3S** in phosphate buffer (pH = 8.0), because this is the optimum pH for enzymes that exhibit polyphenol oxidase activity, such as cresolase and catecholase.[101]

Reaction progress, monitored through the absorption band around 480 nm,[102] depended on the nature of the oxidant and catalyst (Figure 8). Fast fading and low final optical density are characteristic of a highly efficient bleaching system. In turn, an efficient bleaching system can degrade quinones.

During catechol oxidation catalyzed by **CuP1** and **Cu_4CuP3S**, a band arose in the region of 480 nm. The solution changed from colorless to dark brown and then became colorless again, which suggested that the reaction generated quinone and later degraded it.

Meunier et al.[103] conducted a study on catechol oxidation with different oxidants catalyzed by copper phthalocyanines. Oxalic acid (as dimethyl ester, detected by GC-MS), resulting from catechol aromatic ring cleavage, was the final product. The authors described that detailed product analysis was complicated in the case of catechol, because the intermediate *ortho*-quinone polymerized.[103]

Figure 8b shows that, during catechol oxidation, the band at 508 nm diminished along time. The band at 508 nm, typical of the presence of catechol, started to decrease within the first 15 min of reaction, which evidenced catechol conversion into the corresponding quinone.

The absorbance decrease at 508 nm aided determination of the reaction rates. It was possible to obtain good linear plots of ln A/A_0 versus time under the pseudo-first-order conditions, for

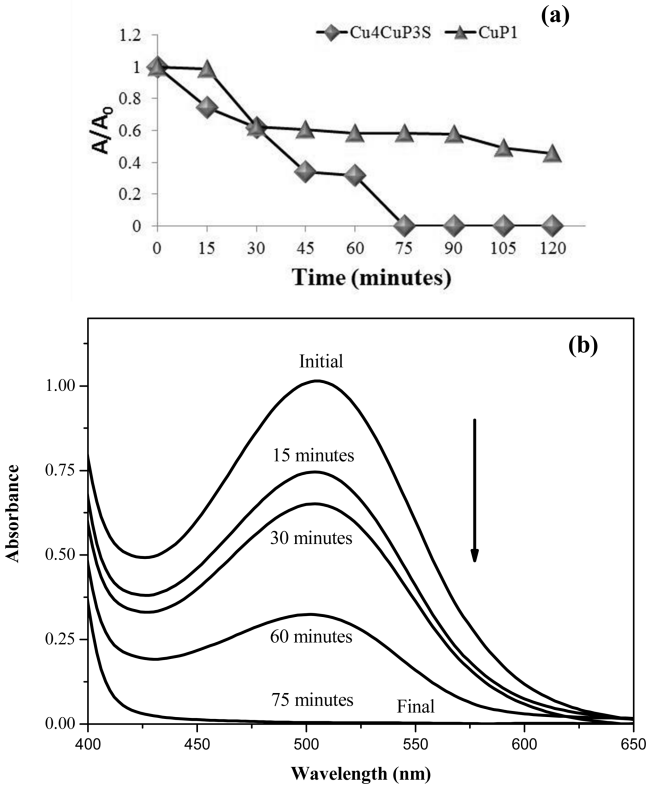

Figure 8. (a) Relation between A/A_0 (where A = final absorbance and A_0 = initial absorbance) and time (minutes). (b) Variation of the absorbance at 508 nm versus time during catechol oxidation catalyzed by Cu_4CuP3S.

a constant H_2O_2 concentration. Calculation of the observed constants (k_{obs}) for each reaction by means of the linearized equation showed that the rates of the noncatalyzed reactions ($k_{obs} = 1.71 \times 10^{-3}$ min^{-1}) were smaller than the rates of the catalyzed reactions (**CuP1** $k_{obs} = 9.68 \times 10^{-3}$ min^{-1} and **Cu_4CuP3S** $k_{obs} = 1.91 \times 10^{-2}$ min^{-1}). **Cu_4CuP3S** gave the best result, which was 10 times greater than k_{obs} achieved for the noncatalyzed reactions and two times greater than k_{obs} obtained for **CuP1**. In other words, **Cu_4CuP3S** was a more effective catalyst for catechol oxidation than **CuP1** under the same reaction conditions. **CuP1** and solid **Cu_4CuP3S** afforded a conversion rate of 41.5% after 90 and 45 min of reaction, respectively. **Cu_4CuP3S** completely converted catechol after 90 min of reaction, while **CuP3** provided a conversion rate of 19.2%.

In the case of catechol oxidation, **CuP1** was poorly soluble in the employed buffer condition. **CuP3** was not completely soluble in the oxidation condition, either, but it was more soluble than **CuP1**. Thus, the higher reactivity of solid **Cu_4CuP3S** as compared with **CuP1** and **CuP3** under heterogeneous conditions indicated that self-assembly of the galactose dendrimer units mediated by the copper ions enhanced **Cu_4CuP3S** stability.

Table 5 brings the results obtained during catechol oxidation as a function of the reaction time. Product yield depended on time when **Cu_4CuP3S** was the catalyst: an increase in reaction time from 15 to 75 min led to almost 100% conversion and raised the product yield and turnover frequency. Conversion percentages rose during the **CuP1**- and **Cu_4CuP3S**-catalyzed reactions as compared with the control reaction.

DOI: 10.1021/acs.inorgchem.5b00196
Inorg. Chem. XXXX, XXX, XXX−XXX

Table 5. Catechol Oxidation to *ortho*-Benzoquinone by H_2O_2 Catalyzed CuP1 or Cu_4CuP3S

	CuP1[a]		Cu_4CuP3S		control[b]
time (min)	conversion[a,c] %	TOF[d] (h^{-1})	conversion[a,c] %	TOF[d] (h^{-1})	conversion[a,c] %
15	1.3	1.3	27.4	29.3	1.2
30	18.3	17.4	35.7	38.3	4.6
45	39.3	38.3	46.2	49.5	6.9
60	40.3	40.5	66.1	70.8	8.7
60 (first reuse)	-	-	56	51.5	-
60 (second reuse)	-	-	54	49.5	-
75	40.9	40.7	98	89.4	11.2
90	41.5	40.9	100	91.5	12.0

[a]The results represent reactions performed in duplicate or triplicate. [b]Reactions performed without catalyst (only hydrogen peroxide and substrate) resulted in low conversion in the employed reaction conditions. [c]Percent conversion was calculated on the basis of the amount of remaining substrate. [d]Turnover frequency (h^{-1}) = number of moles of product per number of moles of catalyst per hour. Turnover frequency was calculated from the reaction rate at 60 min—reactions not performed because the catalyst, which was composed of a very fine powder, was lost during manipulation, washing, and drying, making reuse experiments impossible to perform ("-" means that the reaction was not performed).

Meunier et al.[103] showed that catechol oxidation with hydrogen peroxide catalyzed by iron phthalocyanines gave 38% product yield after 1 h of reaction. Here, solid **Cu_4CuP3S** afforded a much better result, namely, 66% of catechol conversion under the same reaction conditions and after the same reaction time.[103]

Solid **Cu_4CuP3S** completely oxidized catechol after 90 min, a result that was even better than the data reported for other copper complexes, such as copper(II) phthalocyanine immobilized on LDH.[104]

Conducting a reaction that used only copper acetate as catalyst helped to prove that the efficiency of the heterogeneous catalytic process was really due to the copper porphyrin present in solid **Cu_4CuP3S**. In the presence of copper acetate, catechol conversion into *ortho*-benzoquinone was 26% after 2 h of reaction. In the absence of any catalyst, catechol conversion was ca. 10% after 1 h of reaction.

Catalyst reuse in a second cycle after 1 h of reaction showed whether solid **Cu_4CuP3S** was recyclable. In the second use, the product yield changed from 66% to 56%. This relatively small decrease suggested that the porphyrin macrocycle underwent partial damage in the presence of the oxidant or that the catalytic species experienced a rearrangement in the solid structure. In the third use, the yield was practically the same as in the second use (54%), indicating that solid **Cu_4CuP3S** was stable and reusable in other cycles under controlled catalytic reaction conditions.

Catalyst heterogenization on an inert solid (e.g., catalyst immobilization on silica[75,89,105,106] or catalyst transformation into an insoluble solid by synthetic processes, as in the case of solid **Cu_4CuP3S**) effectively minimizes the deactivation effects that may take place during homogeneous catalysis, particularly oxidative catalyst destruction during the catalytic reactions, and improves catalytic performance. The major advantage of solid **Cu_4CuP3S** prepared in this work is that it is insoluble and contains more catalytic species per mass of solid catalyst as compared with the solid resulting from catalyst immobilization on an inert solid. As a consequence, **Cu_4CuP3S** acts as a solid catalyst for heterogeneous processes and is reusable.

4. CONCLUSIONS

Porphyrin **H_2P3**, which bears galactodendritic moieties, affords the new solid porphyrinic material **Cu_4CuP3S** after metalation with excess copper(II) acetate. **Cu_4CuP3S** displays very promising catalytic activity in the oxidation of alkenes, alcohols, and catechol. Treatment of **Cu_4CuP3S** and **CuP3** (obtained by reacting **H_2P3** with 1 equiv of copper acetate) with zinc(II) acetate and characterization of the materials by UV−vis, FTIR, and EPR helped to confirm the presence of copper(II) in the porphyrin macrocycle irrespective of the metalloporphyrin preparation conditions and of the presence of zinc(II).

The fact that solid **Cu_4CuP3S** and solid **Zn_4CuP3S** constitute efficient catalysts in oxidation reactions shows that **Cu_4CuP3S** is a promising catalyst for the oxidation of alkenes, alcohols, and catechol in heterogeneous processes.

Minimization of the catalyst deactivation process typical of homogeneous oxidation catalysis and the possibility of catalyst recovery and reuse are particularly important features of solid **Cu_4CuP3S**.

Reuse of **Cu_4CuP3S** in (*Z*)-cyclooctene and catechol oxidation does not lead to catalyst solubilization during the reactions or the washing processes. This paves the way for investigations into new substrates and different reaction conditions.

■ ASSOCIATED CONTENT

Supporting Information

Synthesis of porphyrins (**H_2P1**, **H_2P2**, and **H_2P3**), characterization (by ^1H NMR, ^{13}C NMR, HRMS-ESI, UV−vis) and UV−vis spectra of the free compounds **H_2P1**, **CuP1**, **H_2P3**, **CuP3**, and **Zn_4CuP3S**. This material is available free of charge via the Internet at http://pubs.acs.org.

■ AUTHOR INFORMATION

Corresponding Authors

#E-mail: jtome@ua.pt. (J.P.C.T.)
*E-mail: shirleyn@ufpr.br. (S.N.)

Notes

The authors declare no competing financial interest.

■ ACKNOWLEDGMENTS

The authors are grateful to Conselho Nacional de Desenvolvimento Científico e Tecnológico (CNPq), Coordenação de Aperfeiçoamento de Pessoal de Nível Superior (CAPES), Fundação Araucária, Fundação da Universidade Federal do Paraná (FUNPAR), and Universidade Federal do Paraná (UFPR) for financial support. Thanks are also given to Fundação para a Ciência e a Tecnologia (FCT, Portugal), the European Union, QREN, FEDER, COMPETE, for funding the Organic Chemistry Research Unit (QOPNA, Project PEst-C/

DOI: 10.1021/acs.inorgchem.5b00196
Inorg. Chem. XXXX, XXX, XXX−XXX

QUI/UI0062/2013; FCOMP-01-0124-FEDER-037296), and to the Portuguese National NMR Network, which also supported by funds from FCT. K.A.D.F.C. also thanks CAPES for the Ph.D. sandwich scholarship (Process 6883-10-9). S.S. and P.M.R.P. thank FCT for their postdoctoral (SFRH/BPD/64812/2009) and Ph.D. (SFRH/BD/85941/2012) grants, respectively.

REFERENCES

(1) Dolphin, D. In: *The Porphyrins;* Academic Press: New York, 1978, *v.1*.
(2) Yamaguchi, H.; Tsubouchi, K.; Kawaguchi, K.; Horita, E.; Harada, A. *Chem.—Eur. J.* **2004**, *10*, 6179−6186.
(3) Bernadou, J.; Meunier, J. *Adv. Synth. Catal.* **2004**, *346*, 171−184.
(4) Mansuy, D. *C. R. Chim.* **2007**, *10*, 392−413.
(5) Appleton, A. J.; Evans, S.; Smith, J. R. L. *J. Chem. Soc., Perkin Trans. 2* **1995**, 281−285.
(6) Ricoux, R.; Raffy, Q.; Mahy, J. P. *C. R. Chim.* **2007**, *10*, 684−702.
(7) Hirohara, S.; Nishida, M.; Sharyo, K.; Obata, M.; Ando, T.; Tanihara, M. *Bioorg. Med. Chem.* **2010**, *18*, 1526−1535.
(8) Moura, N. M. M.; Giuntini, F.; Faustino, M. A. F.; Neves, M. G. P. M. S; Tomé, A. C.; Silva, A. M. S.; Rakib, E. M.; Hannioui, A.; Abouricha, S.; Röder, B.; Cavaleiro, J. A. S. *ARKIVOC* **2010**, 24−33.
(9) Alves, E.; Faustino, M. A. F.; Neves, M. G. P. M. S.; Cunha, Â.; Nadais, H.; Almeida, A. *J. Photochem. Photobiol., C* **2015**, *22*, 34−57.
(10) Costa, L.; Faustino, M. A. F.; Neves, M. G. P. M. S.; Cunha, Â.; Almeida, A. *Viruses* **2012**, *4*, 1034−1074.
(11) Silva, D. C.; Silva, G. F.; Nascimento, E.; Rebouças, J. S.; Barbeira, P. J. S.; Carvalho, M. E. M. D.; Idemori, Y. M. *J. Inorg. Biochem.* **2008**, *102*, 1932−1941.
(12) Shultz, A. M.; Farha, O. K.; Hupp, J. T.; Nguyen, S. T. *J. Am. Chem. Soc.* **2009**, *131*, 4204−4205.
(13) Liang, J.-L.; Huang, J.-S.; Yu, X.-Q.; Zhu, N.; Che, C.-H. *Chem.—Eur. J.* **2002**, *8*, 1563−1572.
(14) Yang, J.; Gabriele, B.; Belvedere, S.; Huang, Y.; Breslow, R. *J. Org. Chem.* **2002**, *67*, 5057−5067.
(15) Cheng, N.; Kemnan, C.; Goubert-Renaudin, S.; Wieckowski, A. *Electrocatalysis* **2012**, *3*, 238−251.
(16) Che, C.-M.; Lo, V. K-L.; Zhou, C.-Y.; Huang, J.-S. *Chem. Soc. Rev.* **2011**, *40*, 1950−1975.
(17) Vlascici, D.; Fadagar-Cosma, E.; Popa, I.; Chiriac, V.; Gil-Agusti, M. *Sensors* **2012**, *12*, 8193−8203.
(18) Moura, N. M. M.; Núñez, C.; Faustino, M. A. F.; Cavaleiro, J. A. S.; Neves, M. G. P. M. S; Capelo, J. L.; Lodeiro, C. *J. Mater. Chem. A* **2014**, *2*, 4772−4783.
(19) Purrello, R.; Gurrieri, S.; Laureci, R. *Coord. Chem. Rev.* **1999**, *683*, 190−192.
(20) Pereira, A. M. V. M; Hausmann, A.; Tomé, J. P. C.; Trukhina, O.; Urbani, M.; Neves, M. G. P. M. S.; Cavaleiro, J. A. S.; Guldi, D. M.; Torres, T. *Chem.—Eur. J.* **2012**, *18*, 3210−3219.
(21) Yella, A.; Lee, H.-W.; Tsao, H. N.; Yi, C.; Chandiran, A. K.; Diau, E. W-G-; Yeh, C.-Y.; Zakeeruddin, S. M.; Grätzel, M. *Science* **2011**, *334*, 629−655.
(22) Poulos, T. L. *Biochem. Biophys. Res.* **2005**, *338*, 337−345.
(23) Isin, E. M.; Guengerich, F. P. *Biochem. Biophys. Acta* **2007**, *1770*, 314−329.
(24) Meunier, B.; Visser, S. P.; Shaik, S. *Chem. Rev.* **2004**, *104*, 3947−3980.
(25) Doro, F. G.; Smith, J. R. L.; Ferreira, A. G.; Assis, M. D. *J. Mol. Catal. A: Chem.* **2000**, *164*, 97−108.
(26) Groves, J. T.; Nemo, T. E.; Myers, R. S. *J. Am. Chem. Soc.* **1979**, *101* (4), 1032−1033.
(27) Simões, M. M. Q.; Paula, R.; Neves, M. G. P. M. S.; Cavaleiro, J. A. S. *J. Porphyrins Phthalocyanines* **2009**, *13*, 589−596.
(28) Halma, M.; Castro, K. A. D. F.; Taviot-Gueho, C.; Prévot, V.; Forano, C.; Wypych, F.; Nakagaki, S. *J. Catal.* **2008**, *257*, 233−243.
(29) Traylor, T. G.; Byun, Y. S.; Traylor, P. S.; Battioni, P.; Mansuy, D. *J. Am. Chem. Soc.* **1991**, *113*, 7821−7823.
(30) Machado, G. S.; Groszewicz, P. B.; Castro, K. A. D. F.; Wypych, F.; Nakagaki, S. *J. Colloid Interface Science* **2012**, *374*, 278−286.
(31) Castro, K. A. D. F.; Bail, A.; Groszewicz, P. B.; Machado, G. S.; Schreiner, W.; Wypych, F.; Nakagaki, S. *Appl. Catal., A* **2010**, *386*, 51−59.
(32) Groves, J. T. *J. Inorg. Biochem.* **2006**, *100*, 434−447.
(33) Koval, I. A.; Gamez, P.; Belle, C.; Selmeczi, K.; Reedijk, J. *Chem. Soc. Rev.* **2006**, *35*, 814−840.
(34) Mayer, A. M. *Phytochemistry* **2006**, *67*, 2318−2331.
(35) Kiralp, S.; Toppare, L.; Yagci, Y. *Des. Monomers Polym.* **2004**, *7*, 3−10.
(36) Neves, A.; Rossi, L. M.; Bortoluzzi, A. J.; Szpoganicz, B.; Wiezbicki, C.; Schwingel, E. *Inorg. Chem.* **2002**, *41*, 1788−1794.
(37) Sharefkin, J. C.; Saltzmann, H. *Org. Synth.* **1963**, *43*, 62.
(38) Gonsalves, A. M. A. R.; Varejão, J. M. T. B.; Pereira, M. M. J. *Heterocycl. Chem.* **1991**, *28*, 635−640.
(39) Silva, S.; Pereira, P. M. R.; Silva, P.; Paz, F. A. A.; Faustino, M. A. F.; Cavaleiro, J. A. S.; Tomé, J. *Chem. Commun.* **2012**, *48*, 3608−3610.
(40) Kobayashi, H.; Higuchi, T.; Kaizu, Y.; Osada, H.; Aoki, M. *Bull. Chem. Soc. Jpn.* **1975**, *48*, 3137−3141.
(41) Sheldon, R. A.; Wallau, M.; Arends, I. W. C. E.; Schuchardr, U. *Acc. Chem. Res.* **1998**, *31*, 485−493.
(42) Waite, J. H.; Tanzer, M. L. *Anal. Biochem.* **1981**, *111*, 131−136.
(43) Goutermann, M. *J. Mol. Spectrosc.* **1961**, *6*, 138−163.
(44) Sebestij, V. J.; Niederhafner, P.; Jezek, J. *Amino Acids* **2011**, *40*, 301−370.
(45) Sinelshchikova, A. A.; Nefedov, S. E.; Enakieva, Y. Y.; Gorbunova, Y. G.; Tsivadze, A. Y.; Kadish, K. M.; Chen, P.; Bessmertnykh-Lemeune, A.; Stern, C.; Guilard, R. *Inorg. Chem.* **2013**, *52*, 999−1008.
(46) Suslick, K. S.; Bhyrappa, P.; Chou, J.-H.; Kosal, M. E.; Nakagaki, S.; Smithhenry, D. M.; Wilson, S. R. *Acc. Chem. Res.* **2006**, *38*, 283−291.
(47) Nakagaki, S.; Ferreira, G. K. B.; Ucoski, G. M.; Castro, K. A. D. F. *Molecules* **2013**, *18*, 7279−7308.
(48) O'Keeffe, M.; Yaghi, O. M. *Chem. Rev.* **2012**, *112*, 675−702.
(49) Li, H.; Eddaoudi, M.; Groy, T. L.; Yaghi, O. M. *J. Am. Chem. Soc.* **1998**, *120*, 8571−8572.
(50) Barron, P. M.; Wray, C. A.; Hu, C.; Guo, Z.; Choe, W. *Inorg. Chem.* **2010**, *49*, 10217−10219.
(51) Ohmura, T.; Usuki, A.; Fukmori, K.; Ohta, T.; Ito, M.; Tatsumi, K. *Inorg. Chem.* **2006**, *45*, 7988−7990.
(52) Nakamoto, K. In *Infrared and Raman Spectra of Inorganic and Coordination Compounds, Parts A & B,* 5th ed.; John Wiley & Sons Inc.: New York, 1997.
(53) Bandgar, B. P.; Gujarathi, P. B. *J. Chem. Sci.* **2008**, *120*, 259−266.
(54) Alston, K.; Storm, C. B. *Biochemistry* **1979**, *18*, 4292−4300.
(55) Keskin, B.; Koseoglu, Y.; Avcata, U.; Gul, A. *Polyhedron* **2008**, *27*, 1155−1160.
(56) Assour, J. M. *J. Chem. Phys.* **1965**, *43*, 2477−2489.
(57) Cunningham, K. L.; Mcnett, K. M.; Pierce, R. A.; Davis, K. A.; Harris, H. H.; Falck, D. M.; McMillin, D. R. *Inorg. Chem.* **1997**, *36*, 608−613.
(58) Nonomura, Y.; Yoshitaka, Y.; Inoue, N. *Inorg. Chim. Acta* **1994**, *224*, 181−184.
(59) Valente, M.; Freire, C.; Castro, B. *J. Chem. Soc., Dalton Trans.* **1998**, 1557−1562.
(60) Mot, A. C.; Syrbu, S. A.; Makarov, S. V.; Damian, G.; Silaghi-Dumitrescu, R. *Inorg. Chem. Commun.* **2012**, *18*, 1−3.
(61) Nakagaki, S.; Xavier, C. R.; Wosniak, A. J.; Mangrich, A. S.; Wypych, F.; Cantão, M. P.; Denicolóc, I.; Kubotad, L. T. *Colloids Surf., A* **2000**, *168*, 261−276.
(62) George, R. G.; Padmanabhan, M. *Polyhedron* **2005**, *24*, 679−684.
(63) Lau, P. W.; Lin, W. C. *J. Inorg. Nucl. Chem.* **1975**, *37*, 2389−2398.
(64) Kivelson, D.; Neiman, R. *J. Chem. Phys.* **1961**, *35*, 149−155.

DOI: 10.1021/acs.inorgchem.5b00196
Inorg. Chem. XXXX, XXX, XXX−XXX

(65) Appleton, A. J.; Evans, S.; Smith, J. R. L. *J. Chem. Soc., Perkin Trans. 2* **1995**, 281−285.
(66) Dolphin, D.; Traylor, T. G.; Xie, L. Y. *Acc. Chem. Res.* **1997**, *30*, 251−259.
(67) Suslick, K. S. In *The Porphyrin Handbook;* Kadish, K., Smith, K., Guillard R, R. R, Eds.; Academic Press: New York, 1999.
(68) Zampronio, E. C.; Gotardo, M. C. A. F.; Assis, M. D.; Oliveira, H. P. *Catal. Lett.* **2005**, *104*, 53−56.
(69) Lima, O. J.; Aguirre, D. P.; Oliveira, D. C.; Silva, M. A.; Mello, C.; Leite, C. A. P.; Sacco, H. C.; Ciuffi, K. *J. Mater. Chem.* **2001**, *11*, 2476−2481.
(70) Groves, J. T.; Nemo, T. E.; Myers, R. S. *J. Am. Chem. Soc.* **1979**, *101* (4), 1032−1033.
(71) *Comprehensive Supramolecular Chemistry;* Suslick, K. S., Ed.; Elsevier Publishers: Oxford, U.K., 1996; Vol. *5*: Bioinorganic Systems.
(72) Nam, W.; Lee, H. J.; Oha, So-Young; Kimb, C.; Jang, H. G. *J. Inorg. Biochem.* **2000**, *80*, 219−225.
(73) Paula, R.; Simões, M. M. Q.; Neves, M. G. P. M. S.; Cavaleiro, J. A. S. *J. Mol. Catal. A: Chem.* **2011**, *345*, 1−11.
(74) Faria, A. L.; Mac Leod, T. C. O.; Assis, M. D. *Catal. Today* **2008**, *863*, 133−135.
(75) Castro, K. A. D. F.; Halma, M.; Machado, G. S.; Ricci, G. P.; Ucoski, G. M.; Ciuffi, K. J.; Nakagaki, S. *J. Braz. Chem. Soc.* **2010**, *21*, 1329−1340.
(76) Inchley, P.; Lindsay-Smith, J. R. *J. Chem. Soc., Perkin Trans. 2* **1995**, 1579−1587.
(77) Smith, J. R. L.; Iamamoto, I.; Vinhado, F. S. *J. Mol. Catal. A: Chem.* **2006**, *252*, 23−30.
(78) Keilin, J. *Biochem. J.* **1951**, *49*, 544−550.
(79) Stotz, E.; Harrer, C. J.; King, C. G. *J. Biol. Chem.* **1937**, *119*, 511−522.
(80) Manassen, J. *J. Catal.* **1974**, *33*, 133−137.
(81) Manassen, J.; Bar-Ilan, A. *J. Catal.* **1970**, *17*, 86−92.
(82) Wolberg, A.; Manassen, J. *J. Am. Chem. Soc.* **1970**, *92*, 2982−2991.
(83) Castro, K. A. D. F.; Simões, M. M. Q.; Neves, M. G. P. M. S.; Cavaleiro, J. A. S.; Ribeiro, R. R.; Wypych, F.; Nakagaki. *Appl. Catal., A* **2015**, in press.
(84) Seelan, S.; Agashe, M. S.; Srinivas, D.; Silvasanker, S. *J. Mol. Catal. A: Chem.* **2001**, *168*, 61−68.
(85) Raja, R.; Ratnasamy, R. *Catal. Lett.* **1997**, *48*, 1−10.
(86) Rahimi, R.; Gholamrezapor, E.; Nami-jamal, M. R. *Inorg. Chem. Commun.* **2011**, *14*, 1561−1568.
(87) Ma, D.; Hu, B.; Lu, C. *Catal. Commun.* **2009**, *10*, 781−783.
(88) Groves, J. T.; Kruper, W. J.; Haushalter, R. C. *J. Am. Chem. Soc.* **1980**, *102*, 6375−6377.
(89) Castro, K. A. D. F.; Simões, M. M. Q.; Neves, M. G. P. M. S.; Wypych, F.; Cavaleiro, J. A. S.; Nakagaki, S. *Catal. Sci. Technol.* **2014**, *4*, 129−141.
(90) Machado, G. S.; Arízaga, G. G. C.; Wypych, F.; Nakagaki, S. *J. Catal.* **2010**, *274*, 130−141.
(91) Hill, C. L.; Schardt, B. C. *J. Am. Chem. Soc.* **1980**, *102*, 6374−6375.
(92) Balahura, R. J.; Sorokin, A.; Bernardou, J.; Meunier, B. *Inorg. Chem.* **1997**, *36*, 3488−3492.
(93) Crawford, P. W.; Carlos, E.; Ellegood, J. C.; Cheng, C. C.; Dong, Q.; Liu, F. D.; Luo, Y. L. *Electrochim. Acta* **1996**, *41*, 2399−2403.
(94) Pinto, A. V.; Ferreira, V. F.; Capella, R. S.; Gilbert, B.; Pinto, M. C.; Silva, J. S. *Trans. R. Soc. Trop. Med. Hyg.* **1987**, *81*, 609−610.
(95) Ribeiro-Rodrigues, R.; Santos, W. G.; Oliveira, A. B.; Snieckus, V.; Zani, C. L.; Romanha, A. J. *Bioorg. Med. Chem. Lett.* **1995**, *5* (14), 1509−1512.
(96) Almeida, E. R.; Filho Silva, A. A.; Santos, E. R.; Lopes, C. A. *J. Ethnopharmacol.* **1990**, *29*, 239−241.
(97) Teixeira, M. J.; Almeida, Y. M.; Viana, J. R.; Filha Holanda, J. G.; Rodrigues, T. P.; Prada, J. R. C., Jr; Coêlho, I. C. B.; Rao, V. S.; Pompeu, M. M. L. *Phytother. Res.* **2001**, *15*, 44−48.
(98) Li, Y. Z.; Li, C. J.; Pinto, A. V.; Pardee, A. B. *Mol. Med.* **1999**, *5*, 711−720.
(99) Gupta, D.; Podar, K.; Tai, Y.-T.; Lin, B.; Hideshima, T.; Akiyama, M.; LeBlanc, R.; Catley, L.; Mitsiades, N.; Mitsiades, C.; Chauhan, D.; Munshi, N. C.; Anderson, K. C. *Exp. Hematol.* **2002**, *30*, 711−720.
(100) Gao, J.; Zhong, S. *J. Mol. Catal.* **2000**, *164*, 1−7.
(101) Martins, L. R.; Souza, E. T.; Fernandez, T. L.; Souza, B.; Rachinski, S.; Pinheiro, C. B.; Faria, R. B.; Casellato, A.; Machado, S. P.; Mangrich, A. S.; Scarpellini, M. *J. Braz. Chem. Soc.* **2010**, *21*, 1218−1229.
(102) Polisel, D. N.; Sinhorini, A. L. C.; Perone, C. A. S. *J. Health Sci. Inst.* **2010**, *28*, 175−180.
(103) Sorokin, A.; Fraisse, L.; Rabion, A.; Meunier, B. *J. Mol. Catal. A: Chem.* **1997**, *117*, 103−114.
(104) Barbosa, C. A. S.; Dias, P. M.; Ferreira, A. M. C.; Constantino, V. L. *Appl. Clay. Sci.* **2005**, *28*, 147−158.
(105) Ferreira, G. K. B.; Castro, K. A. D. F.; Machado, G. S.; Ribeiro, R. R.; Ciuffi, K. J.; Ricci, G. P.; Marques, J. A.; Nakagaki, S. *J. Mol. Catal. A: Chem.* **2013**, *378*, 263−272.
(106) Nakagaki, S.; Ferreira, G. K. B.; Marçal, A. L.; Ciuffi, K. J. *Curr. Org. Synth.* **2014**, *11*, 67−88.

DOI: 10.1021/acs.inorgchem.5b00196
Inorg. Chem. XXXX, XXX, XXX−XXX